Ferromagnetism in cobalt-implanted ZnO

D. P. Norton,[a] M. E. Overberg, S. J. Pearton, and K. Pruessner
Department of Materials Science and Engineering, University of Florida, Gainesville, Florida 32611

J. D. Budai, L. A. Boatner, and M. F. Chisholm
Oak Ridge National Laboratory, Oak Ridge, Tennessee 37831

J. S. Lee, Z. G. Khim, and Y. D. Park
School of Physics, Seoul National University, Seoul 151-747, Korea

R. G. Wilson
Consultant, Stevenson Ranch, California 91381

(Received 10 September 2003; accepted 7 November 2003)

The magnetic and structural properties of cobalt-implanted ZnO single crystals are reported. High-quality, (110)-oriented single-crystal Sn-doped ZnO substrates were implanted at ~350 °C with Co to yield transition metal concentrations of 3–5 at. % in the near-surface (~2000 Å) region. After implantation, the samples were subject to a 5 min rapid thermal annealing at 700 °C. Magnetization measurements indicate ferromagnetic behavior, with hysteresis observed in the M vs H behavior at $T=5$ K. Coercive fields were $\leqslant$100 Oe at this measurement temperature. Temperature-dependent magnetization measurements showed evidence for ordering temperatures of >300 K, although hysteresis in the M vs H behavior was not observed at room temperature. Four-circle x-ray diffraction results indicate the presence of (110)-oriented hexagonal phase Co in the ZnO matrix. From the 2θ full width at half maximum (FWHM) of the Co (110) peak, the nanocrystal size is estimated to be ~3.5 nm, which is below the superparamagnetic limit at room temperature. In-plane x-ray diffraction results show that the nanocrystals are epitaxial with respect to the ZnO host matrix. The magnetic properties are consistent with the presence of Co nanocrystals, but do not preclude the possibility that a component of the magnetism is due to Co substitution on the Zn site in the ZnO matrix. © *2003 American Institute of Physics.* [DOI: 10.1063/1.1637719]

ZnO is a semiconductor for use in ultraviolet light emitters, gas sensors, and transparent electronics.[1–9] The commonly observed residual conductivity in ZnO is n type,[3,4] p-type doping has proven to be difficult to achieve, however.[5–7] Recently, a significant interest has been exhibited in achieving magnetic functionality in ZnO. Transition-metal-doped ZnO has been investigated as a promising dilute magnetic semiconductor for implementing spintronic device concepts. Dietl *et al.*[10] first predicted a Curie temperature of $\geqslant$300 K for Mn-doped p-type ZnO, while electron doping of Fe, Co, or Ni-doped ZnO was predicted to stabilize high-Curie-temperature ferromagnetism.[11,12] Carrier-induced ferromagnetism has been addressed theoretically by others for the case of hole doping of ZnO(Mn),[13,14] while methods for improving p-type doping have also been suggested.[15] Numerous reports of the magnetic properties of transition-metal-doped ZnO have appeared recently.[1,16–21] In particular, Ueda *et al.*[20] reported a Curie temperatures above 300 K for Co-doped ZnO. A key issue is the origin of magnetism. For Co-doped ZnO, there is some evidence that the observed ferromagnetism may be due to Co precipitates instead of carrier-mediated exchange in the ZnO matrix.[22] If the ferromagnetism reflects the formation of a dilute magnetic semiconductor, then this provides an excellent material system for investigating semiconductor-based spintronic device concepts. If the magnetic properties originate from Co nanoprecipitates, there may be opportunities to exploit these, particularly if the orientations of the hard and easy magnetic axes can be tailored as in the case of Co nanoparticles formed in single-crystal Al_2O_3.[23–28]

In this letter, we report on the magnetic and structural properties of bulk ZnO crystals implanted with Co. The ZnO single crystals were doped with Sn during vapor transport growth, yielding an electron concentration of $\sim 10^{18}$ cm^{-3}. These crystals were subsequently implanted with 250 keV Co^+ ions at doses of 3 or 5×10^{16} cm^{-2} into the (110) growth face. The samples were held at ~350 °C during the implantation step to avoid amorphization of the ZnO lattice. The projected range of the implanted ions is ~2000 Å, producing an average transition metal concentration of ~3 or 5 at. %. The samples were subsequently annealed at 700 °C for 5 min under flowing N_2 gas to repair implant damage. The magnetic properties were examined using a Quantum Design SQUID magnetometer.

X-ray diffraction measurements of the Co-implanted samples yielded evidence for hcp Co nanocrystal precipitates that are epitaxial with respect to the ZnO crystal lattice. Figure 1 shows the 2θ-scan parallel to the surface normal. The ZnO (110) peak at $2\theta=56.6°$ is evident in the scan. A broad diffraction peak at $2\text{-}\theta=75.5°$, corresponding to a d spacing of 1.259 Å, is consistent with either hexagonal Co (110) or cubic Co (220). Note that cobalt can exhibit either the hexagonal *ABABAB*... stacking or the fcc cubic structure (stable above 450 °C) with *ABCABC*... stacking. Standard $\theta 2\theta$ x-ray

[a]Electronic mail: dnort@mse.ufl.edu

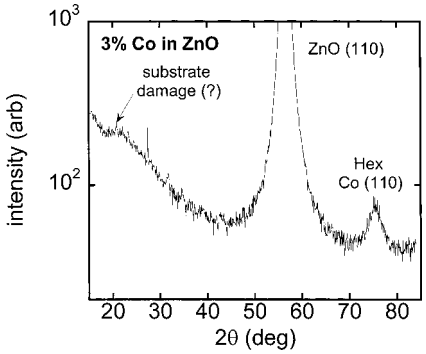

FIG. 1. X-ray diffraction θ-2θ scan for a cobalt-implanted ZnO crystal showing the Co (110) x-ray diffraction peak.

scans do not provide sufficient information to distinguish between the hexagonal and cubic Co structure. The broad shoulder at $2\theta \approx 20°$ likely reflects substrate damage due to the implant. A FWHM in 2θ of 2.9° for the peak at 75.5° corresponds to an x-ray coherence distance (estimate of the nanocrystal size) of 36 Å. This is smaller than the superparamagnetic critical diameter for Co at room temperature, which is relevant to the magnetization measurements.

In order to further investigate the origin of the $2\theta = 75.5°$ peak, four-circle x-ray diffraction was performed. Assuming that the Co peak is hexagonal Co (110), an in-plane scan at $\theta = 49.8°$ would correspond to the hexagonal Co (011). A ϕ scan through the hexagonal Co (011), as shown in Fig. 2(a), reveals two pairs of peaks, one set at $\phi = 44.6°$ and $-135°$, corresponding to a ''hex on hex'' alignment of the Co with ZnO, and a second set at $\phi = -48°$ and 131.5°, which is close to a 90° rotation of the former. In addition, an off-axis diffraction scan parallel to the L axis, but shifted away from the origin, was also performed as shown in Fig. 2(b). Based on the crystal symmetry of the two Co phases, this scan should show peaks at integral L positions for hexagonal stacking and at integer/3 positions for cubic stacking as was demonstrated elsewhere.[29] Figure 2(b) shows an L scan along the Co $(01L)$. The hex Co (01-1) and hex Co (011) peaks are visible, although weak and broad. The hexagonal (001) peak appears too weak to resolve. Most important, there is no evidence for the integer/3 peaks corresponding to the cubic phase. Several attempts were made to verify the orientation, as well as to determine location, of the Co precipitates via transmission electron microscopy. While the images reveal evidence for secondary precipitate formation, we were unable to clearly delineate the nanoparticles microstructure. It also remains to be determined whether the Co nanoparticles segregate to interfaces or to the surface.

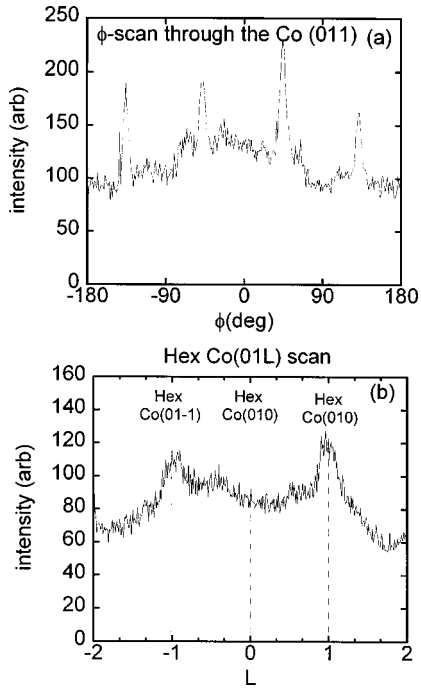

FIG. 2. X-ray diffraction (a) ϕ-scan and (b) L scan indicating that the Co nanocrystals are in-plane aligned and possess the hexagonal structure.

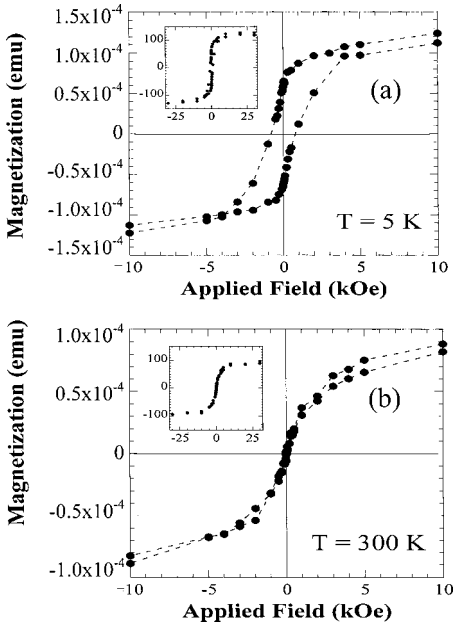

FIG. 3. Magnetization loops at 5 K (top) and 300 K (bottom) for the field applied parallel to the plane of a ZnO sample implanted with 5 at. % Co.

The x-ray diffraction results demonstrate the utility of x-ray diffraction in detecting and identifying precipitate phases in transition metal doped semiconductors. However, if the secondary phases that form are epitaxial, as in the present case, the x-ray diffraction intensity becomes sufficient not only for phase detection in a 2θ scan, but also for in-plane characterization of the phase orientation. In the present case, the Co nanocrystals are epitaxial, thus yielding a unique orientation of both the hard and easy magnetic axes. For the development of nanomagnetic arrays for high-density memory, controlling the orientation of the magnetic axes is critical to maximizing the density of addressable bits. Assuming that the magnetic anisotropy is the same as in the bulk material, the easy axis of the Co nanocrystals is in-plane. More generally, this approach provides a means by which the magnetic anisotropy of the magnetic nanocrystals embedded in a semiconductor matrix can be tailored via selection of the host crystal lattice orientation.

The magnetization behavior of the implanted samples was also investigated. Figure 3 shows magnetization versus field behavior at 5 K (top) and 300 K (bottom) from samples implanted with the 5 at. % dose of Co. Hysteresis is clearly observed at 5 K, with a coercivity <300 Oe. At room temperature, no hysteresis is observed in the magnetization ver-

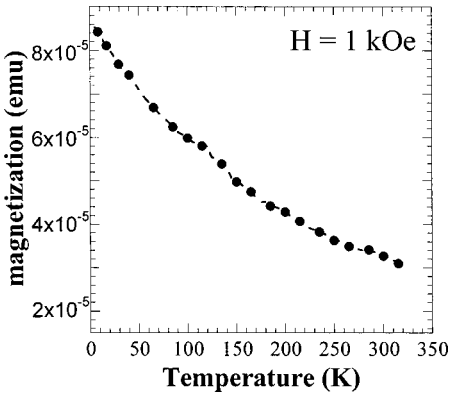

FIG. 4. Temperature dependence of magnetization at a field of 1000 G for a ZnO sample implanted with 3 at. % Co.

sus field data within the resolution of the measurements. Figure 4 shows the temperature dependence of the magnetization from a 3 at. % Co-implanted sample. Unimplanted control samples showed paramagnetic behavior, indicating that the introduction of the Co is the cause of the observed ferromagnetism. Based on the observed magnetization behavior, it is reasonable to assign the magnetic behavior of the implanted samples to the Co nanocrystals detected in x-ray diffraction. Macroscopic Co precipitates would be ferromagnetic with a bulk Curie temperature of 1382 K. However, at ~3.6 nm in diameter, the Co nanocrystals should exhibit superparamagnetic behavior. For hexagonal Co spheres at room temperature, the critical diameter is ~5 nm.[30,31] Based on the x-ray diffraction data, the average size of the Co nanocrystals is below the superparamagnetic limit at room temperature, which is consistent with the magnetic properties observed.

While the presence of Co nanocrystals can account for magnetism in these implanted samples, it does not preclude the possibility that magnetism originating from Co substitution on the Zn sites also contributes. Total energy calculations suggest that Co doping of *n*-type ZnO would produce ferromagnetism.[11] Note that the magnetization is consistent with the disorder model of Bhatt and co-workers.[32–36] Their model takes into account the effects of positional disorder of the magnetic impurities, in which the carriers are allowed to hop only between the transition metal dopants. The interaction between the carriers and the magnetic ions is an antiferromagnetic Heisenberg exchange type. The shape of the $M-T$ plot is a function of the wide distribution of exchange coupling because some transition metal atoms do not order until lower temperatures. While our results are consistent with the theoretical prediction of Sato and Katayama-Yoshida[11] from total energy calculations that indicated Co doping would induce ferromagnetism in *n*-type ZnO, the presence of Co nanocrystals prevents a unique determination as to whether this mechanism is relevant.

The work at UF is partially supported by NSF Grant (DMR-0101856 and DMR-0101438) and by ARO, while the work at SNU is partially supported by KOSEF and Samsung Electronics Endowment through CSCMR. Oak Ridge National Laboratory is managed by UT-Battelle, LLC for the U.S. Department of Energy under Contract No. DE-AC05-00OR22725.

[1] A. Tiwari, C. Jin, A. Kuit, D. Kumar, J. F. Muth, and J. Narayan, Solid State Commun. **121**, 371 (2002).
[2] Z. K. Tang, P. Yu, G. K. L. Wong, M. Kawasaki, A. Ohtomo, H. H. Koinuma, and Y. Segawa, Solid State Commun. **103**, 459 (1997).
[3] D. C. Look, J. W. Hemsky, and J. R. Sizelove, Phys. Rev. Lett. **82**, 2552 (1999).
[4] C. G. Van de Walle, Phys. Rev. Lett. **85**, 1012 (2000).
[5] K. Minegishi, Y. Koiwai, Y. Kikuchi, K. Yano, M. Kasuga, and A. Shimizu, Jpn. J. Appl. Phys., Part 2 **36**, L1453 (1997).
[6] T. Yamamoto and H. Katayama-Yoshida, Jpn. J. Appl. Phys., Part 2 **38**, L166 (1999).
[7] M. Joseph, H. Tabata, and T. Kawai, Jpn. J. Appl. Phys., Part 2 **38**, L2505 (1999).
[8] T. Aoki, Y. Hatanaka, and D. C. Look, Appl. Phys. Lett. **76**, 3257 (2000).
[9] Y. R. Ryu, S. Zhu, D. C. Look, J. M. Wrobel, H. M. Jeong, and H. W. White, J. Cryst. Growth **216**, 330 (2000).
[10] T. Dietl, H. Ohno, F. Matsukura, J. Cibert, and D. Ferrand, Science **287**, 1019 (2000).
[11] K. Sato and H. Katayama-Yoshida, Jpn. J. Appl. Phys., Part 2 **40**, L334 (2001).
[12] K. Sato and H. Katayama-Yoshida, Jpn. J. Appl. Phys., Part 2 **39**, L555 (2000).
[13] K. Sato and H. Katayama-Yoshida, Physica E (Amsterdam) **10**, 251 (2001).
[14] K. Sato and H. Katayama-Yoshida, Mater. Res. Soc. Symp. Proc. **666**, F4.6.1 (2001).
[15] T. Yamamoto and H. Katayama-Yoshida, Jpn. J. Appl. Phys., Part 2 **38**, L166 (1999).
[16] T. Fukumura, Z. Jin, M. Kawasaki, T. Shono, T. Hasegawa, S. Koshikara, S. Koshihara, and H. Koinuma, Appl. Phys. Lett. **78**, 958 (2001).
[17] T. Wakano, N. Fujimura, Y. Morinaga, N. Abe, A. Ashida, and T. Ito, Physica E (Amsterdam) **10**, 260 (2001).
[18] Z. Jin, K. Hasegawa, T. Fukumura, Y. Z. Yoo, T. Hasegawa, H. Koinuma, and M. Kawasaki, Physica E (Amsterdam) **10**, 256 (2001).
[19] S. W. Jung, S.-J. An, G.-C. Yi, C. U. Jung, S.-I. Lee, and S. Cho, Appl. Phys. Lett. **80**, 4561 (2002).
[20] K. Ueda, H. Tabota, and T. Kamai, Appl. Phys. Lett. **79**, 988 (2001).
[21] H.-J. Lee, S.-Y. Jeong, C. R. Cho, and C. H. Park, Appl. Phys. Lett. **81**, 4020 (2002).
[22] J. H. Kim, H. Kim, D. Kim, Y. E. Ihm, and W. K. Choo, J. Appl. Phys. **92**, 6066 (2002).
[23] M. Klimenkov, J. von Borany, W. Matz, D. Eckert, M. Wolf, and K.-H. Müller, Appl. Phys. A: Mater. Sci. Process. **74**, 571 (2002).
[24] M. Sato, S. Takada, S. Kohiki, T. Babasaki, H. Deguchi, M. Oku, and M. Mitome, Appl. Phys. Lett. **77**, 1194 (2000).
[25] S. I. Woods, J. R. Kirtley, S. Sun, and R. H. Koch, Phys. Rev. Lett. **87**, 137205 (2001).
[26] C. Petit, J. Legrand, V. Russier, and M. P. Pileni, J. Appl. Phys. **91**, 1502 (2002).
[27] O. Fruchart, P.-O. Jubert, C. Meyer, M. Klaua, J. Barthel, and J. Kirschner, J. Magn. Magn. Mater. **239**, 224 (2002).
[28] M. Spasove, U. Wiedwald, R. Ramchal, M. Farle, M. Hilgendorff, and M. Giersig, J. Magn. Magn. Mater. **240**, 40 (2002).
[29] J. D. Budai, C. W. White, S. P. Withrow, M. F. Chisholm, J. Zhu, and R. A. Zuhr, Nature (London) **390**, 384 (1997).
[30] C. P. Bean, J. Appl. Phys. **26**, 381 (1955).
[31] D. J. Clerk, *Magnetism: Principles and Applications* (Wiley, Chichester 1995).
[32] M. Berciu and R. N. Bhatt, Physica B **312/313**, 815 (2002).
[33] M. Berciu and R. D. Bhatt, Phys. Rev. Lett. **87**, 107203 (2001).
[34] D. E. Angelescu and R. H. Bhatt, Phys. Rev. B **65**, 075211 (2002).
[35] A. C. Durst, R. N. Bhatt, and P. A. Wolff, Phys. Rev. B **65**, 235205 (2002).
[36] R. N. Bhatt, M. Berciu, M. D. Kennett, and X. Wan, J. Supercond. Inc. Novel Magn. **15**, 71 (2002).